RADIOCARBON AND TRITIUM MEASUREMENTS AT THE GXNU-AMS FACILITY

Hongtao Shen[1,2]* • Dingxiong Chen[1] • Junsen Tang[1,2] • Guofeng Zhang[1] • Li Wang[1] • Linjie Qi[1] • Kaiyong Wu[1] • Xinyi Han[1] • He Ouyang[1] • Ning Wang[1,2] • Xiaojun Sun[1,2] • Ming He[3] • Kimikazu Sasa[4] • Shan Jiang[3]

[1]College of Physics and Technology, Guangxi Normal University, Guilin Guangxi 541004, China
[2]Guangxi Key Laboratory of Nuclear Physics and Nuclear Technology, Guilin Guangxi 541004, China
[3]China Institute of Atomic Energy, Beijing 102413, China
[4]University of Tsukuba, Tsukuba, Ibaraki 305-8577, Japan

ABSTRACT. A single-stage accelerator mass spectrometer (GXNU-AMS) developed for radiocarbon and tritium measurements was installed and commissioned at Guangxi Normal University in 2017. After several years of operational and methodological upgrades, its performance has been continuously improved and applied in multidisciplinary fields. Currently, the measurement sensitivity for radiocarbon and tritium is $^{14}C/^{12}C \sim (3.14 \pm 0.05) \times 10^{-15}$ and $^{3}H/^{1}H \sim (1.23 \pm 0.17) \times 10^{-16}$, respectively, and the measurement accuracy is $\sim 0.6\%$, which can meet the measurement requirements in the nuclear, earth, environmental and life science fields. This study presents the performance characteristics of GXNU-AMS and several interesting application studies.

KEYWORDS: ^{14}C, GXNU-AMS, ^{3}H, low-energy.

INTRODUCTION

Accelerator mass spectrometry (AMS), an innovative detection method based on accelerator and ion detection technology (Muller et al. 1977; Elmore et al. 1987), has the advantages of high sensitivity, small sample consumption, and short measurement time, so it has been widely used in nuclear physics, archaeology, earth science, environmental science, and life science (Shen et al. 2009, 2012, 2013, 2015, 2019). In recent years, the design of AMS has tended to be compact, and construction and operation costs have been significantly reduced (Synal et al. 2007, 2010, 2013). The AMS at Guangxi Normal University (GXNU-AMS) was completed at the end of 2017 and has successfully established ^{14}C and ^{3}H measurements methods (Zhao et al. 2020; Shen and Zhang et al. 2022). Since becoming operational, improvements to beam quality, measurement accuracy, sensitivity, and other parameters have been realized, and GXNU-AMS has become a nuclear physics experiment platform with its own characteristics in the world.

SYSTEM DESCRIPTION OF GXNU-AMS

The GXNU-AMS system of Guangxi Normal University is the first Chinese homemade accelerator mass spectrometer (AMS) jointly developed by Guangxi Normal University and the China Institute of Atomic Energy, as shown in Figure 1. It is composed of a cesium sputtering negative ion source, preaccelerator, injection magnet, electric quadrupole lens, main accelerator, gas stripper, analysis magnet, electrostatic analyzer, and detector, as shown in Figure S1. The ion source and injection system are placed onto a –200 kV high voltage platform and five molecular pump stations are used to maintain the vacuum of the accelerator cavity within 2×10^{-5} Pa. The whole system has a footprint of only 2.5 m × 4.6 m.

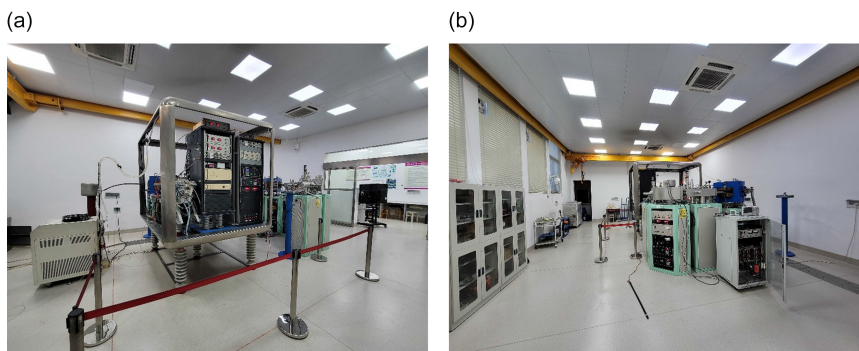*Corresponding author. Email: shenht@gxnu.edu.cn

Figure 1   A single-stage GXNU-AMS system at GXNU.

The ion source is an NEC (National Electrostatics Corp., USA) multitarget (40 targets) cesium sputtering negative ion source. The injected magnet is a double-focusing magnet with a deflection angle of 90° and a deflection radius of 300 mm. An alternating high-frequency potential is applied to the vacuum box in the injection magnet to realize high-speed alternating injection of C isotopes: $^{12}C^-$, $^{13}C^-$, and $^{14}C^-$. An electric quaternary lens focuses the negative-ion beam, which is then accelerated into the gas stripper through a 150-kV accelerating tube. The stripping tube is 500 mm long and has an inner diameter of 10 mm. A 2-mm gas inlet hole is provided in the tube's center to supply helium from an external gas cylinder, and the gas supply is controlled by a high-precision mass flow meter. The stripper gas is extracted by a 600-L turbomolecular pump station installed under the gas stripper. An analysis magnet with a deflection angle of 90º and a deflection radius of 355 mm is used for performing ion momentum/charge selection, then via the electrostatic analyzer with the same deflection angle and a deflection radius of 300 mm for ion energy/charge selection. Finally, the ^{14}C (or ^{3}H) count is recorded by the solid-state detector. Two offset Faraday cups placed at the image points of the injection and analysis magnets are used to simultaneously monitor the beam currents of the stable isotopes at the low-energy and high-energy sides, respectively, and finally, the $^{14}C/^{12}C$ (or $^{3}H/H$) abundance values of the samples are obtained.

SYSTEM PERFORMANCE

The GXNU-AMS system is currently just a homemade non-commercial prototype. Therefore, meticulous fine-tuning of the AMS system is the key to measurement sensitivity and accuracy. The user stabilizes the ion source while monitoring the $^{12}C^-$ (or $^{1}H^-$) beam current in a low-energy (LE) off-axis Faraday cup after setting the ionizer current to 23 A, the oven heater voltage to 23 V (~110ºC), the cathode voltage to 2.5 kV, and the extractor voltage to 13 kV. The typical ^{12}C- and $^{1}H^-$ beam currents at the LE off-axis Faraday cup are 50 µA and 15 µA, respectively. Then, the $^{13}C^-$ (or $^{1}H^-$) beam current is injected through the accelerator, gas stripper, HE magnet, ESA, and finally into the Faraday cup before the detector. By maximizing the beam current by setting the major elements of the machine, the highest possible transmission efficiency is obtained. The overall beam transmission efficiency from the LE Faraday cup to the detector is currently approximately 50% and 85% for ^{12}C and ^{1}H, respectively, and the loss is mainly caused by the loss of charge-state yield at the stripper. Then, moving both magnets to the ^{14}C (or ^{3}H) settings leads to a peak
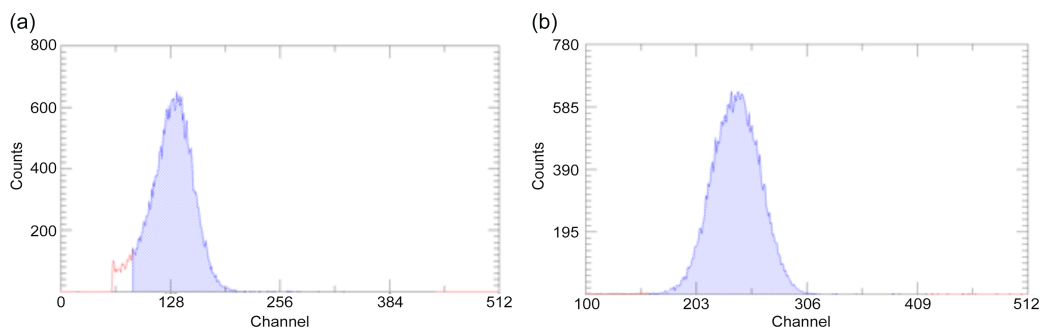
(a)

(b)

Figure 2   Energy spectra of $^{14}C^+$ (a) and $^3H^+$ (b) of semiconductor detectors.

in the ^{14}C (or ^{3}H) count rate measured at the silicon detector. The magnetic component settings should be continuously adjusted to obtain the "flat-top" characteristic curve, as shown in Figure S2, and the final $^{14}C/^{12}C$ (or ^{3}H/H) ratios obtained using a standard should be observed. To ensure the stability of the beam transmission efficiency after running the device for an extended period, we locate the working parameters of each magnetic component at the central position of its "flat-top" curve. Currently, the detection count rate of the GXNU-AMS for the ^{14}C OXII standard and ^{3}H (4.83×10^6 TU) standard samples is approximately 120 counts/s and 200 counts/s, respectively, as shown in Figure 2.

^{14}C Measurement Performance

To verify the ^{14}C measurement performance of GXNU-AMS, we measured a series of international standard samples equivalent to approximately 1 mg of C with known pMC, i.e., OXII (134.07 pMC), IAEA-C7 (49.53 pMC), IAEA-C8 (15.03 pMC), IAEA-C1 (0.00 pMC) and commercial blank graphite to confirm the reliability of GXNU-AMS, as shown in Figure 3, where pMC represents the percentage of modern carbon. Nine 5-minute runs were performed for each sample. The abundance values and uncertainties are based on the average values and the relative standard deviations for five runs, respectively. The measurement results of the standard samples are in line with the nominal values, as shown in Figure 3(a), verifying the reliability of the AMS system. The background value of unprocessed commercial graphite is 0.27 ± 0.02 pMC, as shown in Figure 3(b), and the $^{14}C/^{12}C$ value is $(3.14 \pm 0.05) \times 10^{-15}$, equivalent to a ^{14}C age of approximately 47,000 years. The background value of the process blank ranges between 0.49 pMC and 0.62 pMC, as shown in Figure 3(c), the mean value is 0.55 ± 0.04 pMC, and the $^{14}C/^{12}C$ ratio is $6.47 \pm 0.48 \times 10^{-15}$, which is equivalent to a ^{14}C age of approximately 40,500 years. In addition, international standard samples, such as OXII and IAEA-C8, were prepared and measured using AMS. The average pMC of oxalic acid is determined to be 134.11 ± 0.41 pMC, which is consistent with the recognized standard value of 134.07 pMC within the allowable error. The pMC value of IAEA-C8 is 15.17 ± 0.22 pMC, which is also consistent with the recognized standard value of 15.03 pMC. Moreover, the precision of the system varies by ~0.6% from the test results of standard samples in different time periods, as shown in Figure 3(d), indicating that the system has the high measurement accuracy and proven stability required for environmental and life sciences applications.
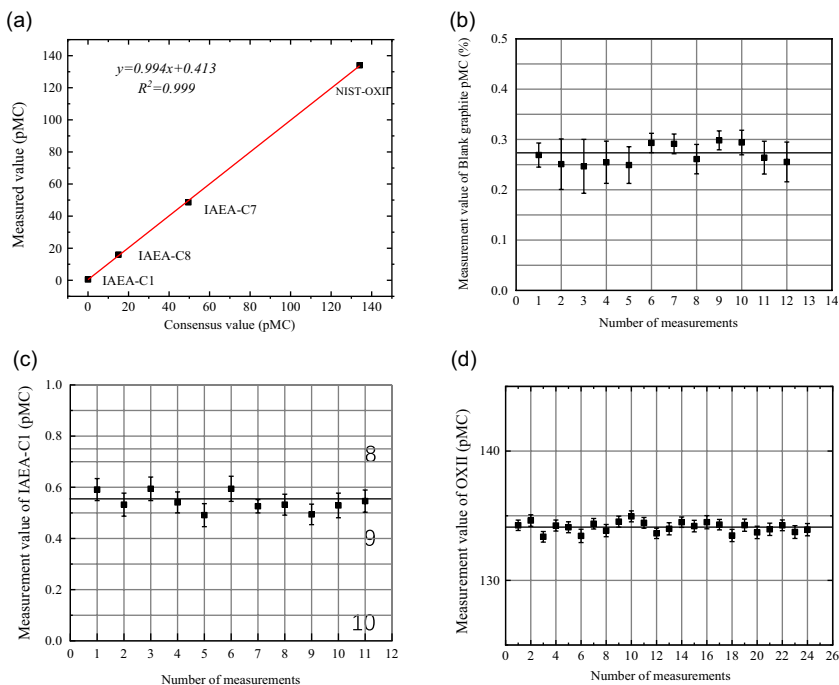
Figure 3   Measurement values of standard and blank samples. (a) Linear relationship between the measured value and nominal value, (b) blank graphite, (c) IAEA-C1, and (d) OXII.

^{3}H Measurement Performance

A series of tritium water samples with a concentration gradient, as shown in Table 1: $1^\#$ (4.55×10^7 TU), $2^\#$ (4.83×10^6 TU), $3^\#$ (5.37×10^5 TU), $4^\#$ (5.46×10^4 TU) and Alfa's commercial TiH_2 (0.00 TU), where 1 Tu represents $^3H/^1H = 1 \times 10^{-18}$, were used as standard and background samples to check the ^{3}H measurement performance of GXNU-AMS. The tritium water standard samples were prepared into titanium hydride by a laboratory vacuum line system (Shen and Tang et al. 2022) and then measured using the GXNU-AMS system. The measurement results of the standard samples are in line with the nominal values, as shown in Figure 4, verifying the reliability of the AMS system for tritium samples. The background ^{3}H/H ratio value of unprocessed commercial TiH_2 is (1.23 ± 0.17) $\times 10^{-16}$ (123TU), as shown in Figure 4.

Performance Comparison of the Commercial AMS

Over the past decade, commercial AMS device design has gradually moved toward compact, low cost, and standardization. The NEC company first introduced an AMS system (SSAMS) of a single-stage electrostatic accelerator with a terminal voltage of 250kV (Schroeder et al. 2007; Skog et al. 2007). The AMS Laboratory at ETH Zurich, Switzerland, in collaboration with Ionplus, then developed a new type of tandem AMS system (MICADAS) with a 200 kV terminal voltage (Synal et al. 2007; Christl et al. 2013). In recent years, HVEE has developed a 200 kV small C-dedicated AMS (Scognamiglio et al. 2021). In 2017, Guangxi Normal University, in collaboration with the China Institute of

Table 1 Results of AMS measurements of standard and blank samples of tritium.

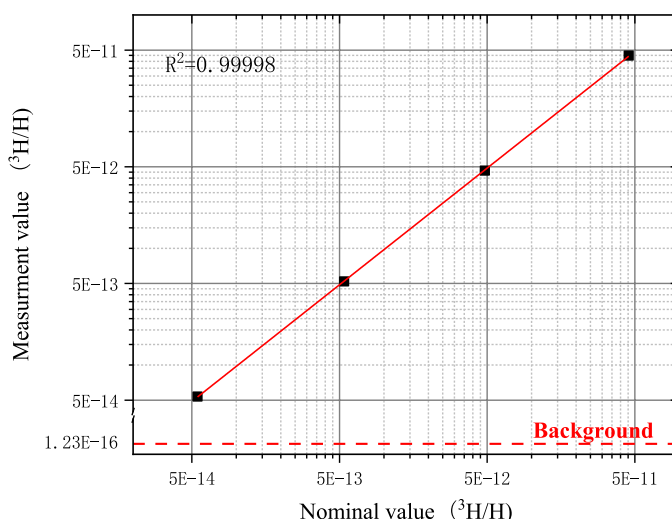| Name	Sample description	Caculated value (TU)	Measured value (TU)
1#	Tritium water (5.426×10^6 Bq/L)	4.55×10^7 TU	$(4.47 \pm 0.05) \times 10^7$ TU
2#	1.072 g of sample 1# + 9.024 g of pure water	4.83×10^6 TU	$(4.63 \pm 0.03) \times 10^6$ TU
3#	1.127 g of sample 2# + 9.022 g of pure water	5.37×10^5 TU	$(5.21 \pm 0.05) \times 10^5$ TU
4#	1.069 g of sample 3# + 9.077 g of pure water	5.46×10^4 TU	$(5.37 \pm 0.09) \times 10^4$ TU
5#	TiH_2	0.00 TU	$(1.23 \pm 0.17) \times 10^2$ TU

Figure 4 Linear relationship between the measured value and nominal value of tritium water containing different $^{3}H/H$ concentrations.

Atomic Energy (CIAE), developed a new 150 kV single-stage AMS (GXNU-AMS) prototype and continuously improved its beam quality, measurement accuracy, sensitivity, and other parameters in the following years. Currently, the main parameters for GXNU-AMS are close to the international level for the same type of commercial AMS, as shown in Table 2.

RESEARCH APPLICATION

Oil Field Tracer Experiment

Zhongyuan Oilfield, Sinopec, central China, has been developed for more than 30 years since 1979. The average comprehensive water cut (the water content in reservoir fluids)of the whole oilfield has reached 86.1%, while the oil recovery is only 21.5%. Especially after years of intense injection and production in the old oilfield, the phenomenon of large pores is widespread in most blocks, seriously threatening the stable production development of the Zhongyuan Oilfield. To overcome these difficulties and scientifically guide extraction in the middle to

Table 2   Technical characteristics of commercial AMS.

Technical parameters	NEC, USA (SSAMS)	Ionplus, Switzerland (MICADAS)	HVEE, Netherlands (4102Bo-AMS)	GXNU-AMS, China
Terminal voltage (kV)	250	200	200	150
Transfer efficiency	43%	47%	50%	50%
Background	2×10^{-15}	$< 1 \times 10^{-15}$	1.5×10^{-15}	3×10^{-15}
Precision	~0.2%	~0.2%	~0.2%	~0.6%
Beam current for $^{12}C^-$ (µA)	50–100	50–100	50–100	~50
Size (m)	5.3×4.2	2.5×3.0	3.1×2.8	2.5×4.5
Type of accelerator	Single-stage	Tandem	Tandem	Single-stage
Measurement nuclides	^{14}C	^{14}C	^{14}C	^{14}C & ^3H

late development stages, we developed a ^{14}C cross-well tracer monitoring technology and applied it to monitor the development status and recognize the heterogeneity of oil reservoirs (Shen and Shi et al. 2022). In this work, the target-well group included one water well (Hu136-C1) and two oil wells (H136-2, H136-8). After the on-site tracer injection of a total dose calculated to be 3.08×10^{18} ^{14}C atoms in this tracer experiment, and using 360 µCi of ^{14}C in the form of commercial urea enriched to 99% in ^{14}C, sampling was started in the two production oil wells on the following days. Approximately 1000 mL of oil-water samples were taken once per day, with this sampling appropriately increased when a tracer was found. After all the peaks were observed, the sampling frequency was gradually reduced from 1 time/2 d to 1 time/4 d to extend the sampling time until the sampling was stopped. The tracer concentrations for the production wells were measured by AMS from October 30, 2020, to March 27, 2021. The monitoring period was 149 days and 298 samples, and the tracer concentration production curves for both production wells are shown in Figure S3. The output curve clearly shows the presence of the tracer on the 20th day in the H136-2 well, and the concentration peak occurs on the 65th, 77th, and 127th days. For the H136-8 well, the tracer is observed on the 54th day, and the peak occurs on the 92nd and 135th days. From these data, the different formation parameters, such as water drive speed, swept volume, permeability, and radius of pore passages, under different well were derived (Shen and Shi et al. 2022). The AMS measurement data also show that the background ^{14}C/^{12}C ratio of the oil-water samples is approximately 5×10^{-14}, the peak ^{14}C/^{12}C ratio is approximately 4×10^{-12} (800 Bq/kg C), which is consistent with our previous calculation, and were used to model underground reservoir characteristics (Wei 2021). It is experimentally verified that ^{14}C-labeled urea is an ideal tracer for cross-well monitoring.

Dating of Chinese Ancient Tea Trees

The jungles of Linyun and Longlin Autonomous Prefecture, located in the heart of the southwestern Guangxi Zhuang Autonomous Region of China, are home to the oldest tea trees (Camellia sinensis) in the world. In the absence of regular annual rings, radiocarbon dating is one of the most powerful tools for assisting in the determination of the ages and growth rates of these plants. In this work, cores were extracted from large ancient tea trees in a central Longlin rainforest; carbon extraction was performed, and the ^{14}C levels in the tree cores were measured using AMS at GXNU (Chen et al. 2019). These measurements indicated that contrary to conventional views, ancient Chinese tea trees appear to commonly reach ages that are rarely attained by any other shrub tree. For the tens of ancient trees sampled, the calibrated age ranges from 300 to 700 years, putting them in the era from the Chinese Qing Dynasty to the Yuan Dynasty. All trees with a diameter at breast height (dbh) >25.0 cm were found to be older than 350 years, and the oldest tree dated by ^{14}C had a dbh of 57.32 cm with an age of 682 years (Table 3).

The age versus tree size (diameter at dbh) relationship is plotted in Figure S4 (a), and the tree size is found to be significantly correlated with age ($P<0.001$). The mean error for the age of ancient tree samples is approximately 40 yr, with a range of 30–50 yr. The age versus growth rate is calculated from the age of the tree center, and the tree diameter is also plotted, as displayed in Figure S4 (b). The mean growth rate is highly correlated with age ($P<0.001$), but the relationship is nonlinear. With an increase in age, the long-term growth rate decreases slowly before finally reaching a balanced value of approximately 0.039 cm yr^{-1}, which is less than the average growth rate for all trees studied in Figure S4 (a), including

Table 3　Data sheet for Chinese ancient tea tree dating.*

Wood sample ID	Fraction modern		^{14}C ages (yr BP)		Tree diameter at dbh (cm)	Mean growth rate (mm yr^{-1})	Cal AD range 2 S.D. (95.4%)[a]	Calibrated cal age (cal yr BP)		Tree age (yr)[b]	
	Best est.	1 S.D.	Best est.	1 S.D.				Best est.	2 S.D.	Best est.	2 S.D.
1#–Longlin	0.931	0.28%	575	23	51.6	0.38	1308–1362 (61.4%) 1386–1416 (34.0%)	615	27	681	27
2#–Longlin	0.966	0.22%	274	18	28.0	0.38	1520–1592 (42.3%) 1622–1665 (51.4%) 1784–1794 (1.7%)	306	22	372	22
3#–Longlin	0.961	0.26%	323	22	39.5	0.42	1488–1604 (75.2%) 1610–1643 (20.2%)	404	58	470	58
4#–Longlin	0.964	0.28%	298	23	32.8	0.36	1499–1502 (0.5%) 1513–1600 (67.9%) 1616–1652 (27.0%)	393	44	459	44
5#–Longlin	0.927	0.26%	605	22	57.3	0.42	1298–1370 (74.3%) 1379–1404 (21.1%)	616	36	682	36
9#–Llingyun	0.961	0.28%	321	23	27.4	0.29	1490–1603 (75.3%) 1612–1644 (20.1%)	403	57	469	57
10#–Llingyun	0.983	0.24%	138	20	23.9	0.41	1670–1779 (41.6%) 1798–1891 (38.2%) 1908–1943 (15.6%)	225	55	291	55
11#–Llingyun	0.967	0.30%	271	25	39.2	0.53	1520–1578 (37.6%) 1582–1591 (1.6%) 1623–1667 (52.4%) 1783–1796 (3.8%)	305	22	371	22
13#–Llingyun	0.981	0.27%	156	22	20.8	0.39	1666–1706 (16.4%) 1720–1784 (37.6%) 1832–1882 (12.1%) 1914– (18.7%)	198	32	264	32
15#–Llingyun	0.970	0.28%	247	23	26.1	0.36	1528–1550 (4.2%) 1633–1670 (66.1%) 1780–1800 (22.9%) 1943– (2.3%)	298	19	364	19

*Abbreviations: AD is Anno Domini; BP is before present, i.e., before AD 1950; and ^{14}C years BP is the radiocarbon-dated years before AD 1950.

[a]The highest probability 2σ range for each sample is given in bold type. The relative areas of 2σ ranges for a radiocarbon date correspond to the 95.4% confidence interval.

[b]The tree ages were calculated from the calibrated cal BP ages extrapolated (from AD 1950) to AD 2016.

the younger known age trees and is a considerably better value for predicting the age of ancient trees with ages >250 yr. Growth rates for tea trees also vary as a function of dbh. For all data combined, the mean growth rate slightly decreases with size up to approximately 20 cm dbh (>250 yr age). Based on this study, we believe that the ^{14}C dating method is effective for determining the lifespan of long-lived trees, such as tea trees, when a given tree is more than 250 years old. The error in the age (30–50 yr) is small enough to determine the estimated lifespan of this species. This study is the first attempt to estimate the mean radial growth rate of ancient Chinese tea trees by applying ^{14}C dating.

Other Applications

The age or retention time of groundwater is closely related to the recharge process of groundwater, which is the embodiment of the exchange of water between aquifers and the external water system, and the process of internal material transport, reflecting the renewability of the aquifer and is also an important indicator of groundwater resource management. The current results show that groundwater dissolved inorganic carbon ^{14}C, with a half-life of 5700 years, is more effective in identifying the age of groundwater formed since 35,000, so it can be used to study the groundwater age for many sedimentary basins. In this work, a new water sample preparation system was developed for accelerator mass spectrometry ^{14}C dating (Qi et al. 2021; Shen and Tang et al. 2022), and a scientific research project based on the determination of groundwater age by AMS in the Xinjiang region, China, was carried out. More than 40 samples were analyzed in the preliminary work, and the age of determination ranged from 3000 to 20,000 years. This study provides a solution for the study of groundwater age and the groundwater pattern environment in a sedimentary basin. Moreover, a special test and analysis of the ^{14}C and ^3H content in the graphite hot column of China's first heavy water research reactor (the 101 reactor) were carried out in cooperation with the CIAE, the result of which provides an essential reference for the design, research, and development of new reactors, new components and new materials in China, as well as the operation management, aging and life evaluation of nuclear facilities and equipment using these materials. These results further confirm the success and reliability of the GXNU-AMS and the measurement method.

CONCLUSION

GXNU-AMS, the first Chinese homemade single-stage AMS system, is in the steady-operation stage after almost five years of operational and methodology upgrades. Currently, the system measurement accuracy is approximately 0.6%, with a $^{14}C/^{12}C$ background of $\sim3 \times 10^{-15}$ (approximately 47000 years) and a $^3H/H$ background of $\sim1 \times 10^{-16}$ and has achieved several significant applications in research with local characteristics, including oilfield tracer technology, dating of ancient Chinese tea trees, and dating of groundwater. In the future, GXNU-AMS will follow a fully open and efficient operation mechanism and will be developed into an open AMS facility that serves the nuclear, earth, environmental and life science fields, leading to a highly advanced and accessible scientific research platform in western China.

ACKNOWLEDGMENTS

SUPPLEMENTARY MATERIAL

To view supplementary material for this article, please visit https://doi.org/10.1017/RDC.2023.31

REFERENCES

Chen J, Shen H, Sasa K, Lan H, Matsunaka T, Matsumura M, Takahashi T, Hosoya S, He M, He Y, et al. 2019. Radiocarbon dating of Chinese ancient tea trees. Radiocarbon 61(6):1741–1748.

Christl M, Vockenhuber C, Kubik PW, et al. 2013. The ETH Zurich AMS facilities: performance parameters and reference material. Nuclear Instruments and Methods in Physics Research B 2013(294):29–38.

Elmore D, Phillips F. 1987. Accelerator mass spectrometry for measurement of long-lived radioisotope. Science 236:543–550.

Muller RA. 1977. Radioisotope dating with a cyclotron. Science 196:489–494.

Qi M, Li Z, Tang, et al. 2021. Development and properties of AMS-^{14}C sample preparation system. Journal of Isotopes 34(3):273. doi: 10.7538/tws.2021.34.03.0273. In Chinese.

Schroeder JB, Hauser TM, Klody GM, et al. 2007. Initial results with low energy single stage AMS. Radiocarbon 46(1):1–4.

Scognamiglio G, Klein M, et al. 2021. Low-energy ^{14}C and multi-element HVE AMS systems. Nuclear Instruments and Methods in Physics Research B 492:29–33.

Shen H, Jiang S, He M, et al. 2012. Measurement of fission product nuclide ^{126}Sn with accelerator mass spectrometry based on SnF$_2$ target, Atomic Energy Science and Technology 46(2):155–159.

Shen H, Jiang S, He M, et al. 2013. AMS measurements of fission products at CIAE. Nuclear Instruments and Methods in Physics Research B 294:136–142.

Shen H, Pang F, Jiang S, He M, Dong K, Dou L, et al. 2015. Study on ^{41}Ca-AMS for diagnosis and assessment of cancer bone metastasis in rats. Nuclear Instruments and Methods in Physics Research B 361:643–648.

Shen H, Ruan X, Jiang S, et al. 2009. Study on calcium net absorptivity by ^{41}Ca labeling calcium pool of rats. Bone 44:60.

Shen H, Sasa K, Meng Q, Matsumura M, Matsunak T, et al. 2019. Exposure age dating of Chinese tiankengs by ^{36}Cl-AMS. Nuclear Instruments and Methods in Physics Research B 459: 29–35.

Shen H, Sasa K, Meng Q, et al. 2019. Cl-36 preparation method for Chinese Karst samples (Tiankeng). Nuclear Instruments and Methods in Physics Research B 458:126–129.

Shen H, Shi S, Tang J, et al. 2022. ^{14}C-AMS technology and its applications to an oil field tracer experiment. Radiocarbon 64(5):1159–1169.

Shen H, Tang J, Wang L, Qi M, et al. 2022. New sample preparation line for radiocarbon measurements at the GXNU laboratory. Radiocarbon 64:1501–1511.

Shen H, Zhang G, Tang J, et al. 2022. A single-stage accelerator mass spectrometer and its applications at Guangxi Normal University. Nuclear Instruments and Methods in Physics Research B 532:68–72.

Synal HA, Stocker M, Suter M. 2007. MICADAS: a new compact radiocarbon AMS system. Nuclear Instruments and Methods in Physics Research B 259(1):7–13.

Synal HA, Wacker L.2010. AMS measurement technique after 30 years: Possibilities and limitations of low energy systems. Nuclear Instruments and Methods in Physics Research B 268 (7–8):701–707.

Synal HA. 2013. Developments in accelerator mass spectrometry. International Journal of Mass Spectrometry 349–350:192–202.

Skog G. 2007. The single stage AMS machine at Lund University: status report. Nuclear Instruments and Methods in Physics Research B 259:1–6.

Wei S. 2021. Study on interwell tracer monitoring interpretation model in oil field [master's dissertation]. Guangxi Normal University. In Chinese.

Zhao Z, Qin Y, Li J, et al. 2020. Experimental conditions of ^{14}C accelerator mass spectrometer. Journal of Chinese Mass Spectrometry Society 41(5):462. In Chinese.